GNS
SCIENCE
TE PŪ AO

# Age constraints on unstable landforms at a near-fault site in Central Otago, New Zealand: Groundwork for validation of Seismic Hazard Models

M. Stirling A. Zondervan
R. Norris D. Ninis

GNS Science Consultancy Report 2009/74
March 2009

**CONFIDENTIAL**



**BIBLIOGRAPHIC REFERENCE**

Stirling, M.; Zondervan, A.; Norris, R.; Ninis, D. 2009. Age constraints on unstable landforms at a near-fault site in Central Otago, New Zealand: Groundwork for validation of Seismic Hazard Models, *GNS Science Consultancy Report* 2009/74. 20p.

Project Number: 430W1297
EQC Project Number: 08/555

# CONTENTS



# FIGURES



# TABLES



# APPENDICES

## NON-TECHNICAL ABSTRACT

Earthquake hazard analysis uses past earthquake activity to forecast future activity. The written and instrumental record of past earthquakes and the prehistorical record of (paleo) earthquakes are used as a basis for estimating the future likelihood of earthquake occurrence and associated strong ground motions. This is the fundamental basis of earthquake hazard analysis. However, the main issue concerning earthquake hazard methodologies is the lack of ability to validate the resulting hazard estimates. Validation involves the use of some independent dataset or observations to gain confidence in the hazard estimates.

Our EQC-funded research project has been focussed on developing methods to validate the very strong earthquake motions predicted at sites near active faults by seismic hazard models in New Zealand. Earthquake motions are expected to be very strong near a causative fault (e.g. ground accelerations of greater than 1g, g being the unit of gravitational acceleration 10m/sec$^2$), but a number of recent large earthquakes (e.g. Chi-Chi, Taiwan) have exhibited motions considerably less than expected. Furthermore, studies in the arid western USA have identified fragile geomorphic features (precariously-balanced rocks, or PBRs) near the San Andreas Fault that have remained unchanged for 10,000 to 100,000 years. The ground motions have not been strong enough to destroy the fragile features, and this provides a valuable constraint on past ground motions. The objective of our EQC-funded research has been to apply these arid western USA studies to a near-fault site in the more humid temperate New Zealand environment. Numerous bedrock (schist) PBRs are present within 5km of the Dunstan Fault in central Otago, a fault capable of generating large earthquakes every 8,000 years on average. Our earlier EQC-funded work showed the PBRs to be too fragile to have survived the ground motions predicted for Dunstan Fault earthquakes from the national seismic hazard model. Either the ground motions have not been as strong as predicted, or the PBRs are too young to have experienced any such earthquakes. Since our earlier studies did not provide adequate age control for the PBRs the present study has largely focussed on this aspect.

We obtained exposure age data for 11 rock samples from one of the PBRs near the Dunstan Fault and from neighbouring features, and have extensively analysed the data. The data provide bedrock erosion rate estimates of about 0.5cm per 1,000 years for the PBRs. This means that they would have been considerably larger and more stable at the start of the Holocene (Holocene is the epoch that spans 10,000 years ago to the present), and therefore not experienced any Dunstan Fault earthquakes in the present fragile state, given the long time period between earthquakes on the fault. The main conclusion of our study is that PBRs in the humid-temperate environment of New Zealand are considerably younger than their arid counterparts, and thus of limited use for constraining near-fault ground motions in areas where large earthquakes do not occur for many thousands of years. Future New Zealand-based efforts should therefore move to studying fragile geomorphic features close to faults that produce large earthquakes more often (i.e. every 100 to 1,000 years). Lastly, the main international contribution arising from our results is that we have provided the first-ever constraints on the age of PBRs in a humid-temperate environment, and that these constraints may be more applicable to similar environments in the USA (e.g. Pacific Northwest) than results obtained from nearby arid environments.

## TECHNICAL ABSTRACT

We constrain the age of precariously-balanced rocks (PBRs) within a metamorphic terrane and temperate environment using in-situ cosmogenic isotopes and geomorphic interpretation. Previous PBR age-related studies have been almost exclusively restricted to arid environments in the western USA. Cosmogenic in-situ 10Be concentrations from 11 samples of schist and silcrete from one PBR site in the central Otago region of New Zealand imply rock surface erosion rates of the order 0.5cm/kyr, consistent with rates of landform evolution and catchment denundation determined elsewhere in the region. The PBRs may only have reached their precarious state less than 10kyr ago, and may not have experienced any earthquakes on the nearby Dunstan Fault, given the long recurrence interval of the fault (8kyr). Future New Zealand-based efforts should therefore move to studying fragile geomorphic features close to faults with much shorter recurrence intervals (100-1,000 years). The main international contribution arising from our results is that PBRs from metamorphic terranes in humid-temperate environments similar to that of central Otago (e.g. parts of central California and Pacific Northwest) may be considerably younger than counterparts in the arid western USA.

# 1. INTRODUCTION

Precariously-balanced rock (PBR) is the name given to a boulder that balances unstably on a pedestal (Fig. 1). PBRs are formed by aeolian, fluvial and chemical weathering of bedrock to produce rock outcrops, along with gradual sculpting of the rock outcrop by weathering processes over time (Fig. 1). Actual PBR formation is achieved when the weathering progresses to the extent that the top of an outcrop is dislocated from the pedestal to form an unstably balanced rock (Step 4 in Fig. 1). The PBR may then become increasingly unstable with time if continued weathering narrows the contact area between pedestal and PBR (compare Steps 4 and 5 in Fig. 1). PBRs were originally so named by Brune (1996) to identify rocks unstable enough to be shaken down by relatively low levels of earthquake shaking (peak ground accelerations, or PGAs of less than 0.2g). Not surprisingly, they have been recognised as having potential for testing seismic hazard models at specific sites for time periods considerably longer than those of historical records (Brune, 1996). Considerable efforts have been focussed on using PBRs to constrain seismic hazard models in the arid western USA where PBRs have been shown to have been precarious for 10 – 100kyrs (e.g. Bell et al. 1998; Purvance et al. 2008).

This report documents research undertaken to extend the PBR studies outside of the arid western USA, by quantifying the age of PBRs in a humid-temperate environment. In this case our research is focussed on a near-fault site in the central Otago region of New Zealand. The study has the objective of applying the largely arid western USA-based PBR methodology (e.g. Bell et al. 1998; Purvance et al. 2008) to a different climatic and geologic environment to determine whether PBRs have a wider applicability, despite radical differences in consequent geomorphic processes. The other important potential benefits are in constraining seismic hazard estimates at near fault sites, and for validating the New Zealand seismic hazard model (e.g. Stirling et al. 2002).

Our work is focussed specifically on reducing the large age uncertainties for schist PBRs reported in a pilot study at a near-fault site in the central Otago province (Fig 2; Stirling & Anooshehpoor 2006). The pilot study made some preliminary comparisons of PBR fragilities (estimates of PGAs required to topple the PBRs) and limited PBR age data (i.e. only two $^{10}$Be cosmogenic exposure ages obtained) to seismic hazard curves (i.e. estimates of expected earthquake ground motion strength as a function of return period). The seismic hazard curves were derived from the New Zealand seismic hazard model (Stirling et al. 2002) for the Clyde site (Fig. 2). The Dunstan Fault is less than 5km from the site (Fig. 2), and the southwestern section of the fault has been assigned a recurrence interval of 8kyr for magnitude (M)7 earthquakes in the national seismic hazard model (Stirling et al. 2002). The Stirling & Anooshehpoor (2006) study suggested a major discrepancy between the seismic hazard estimates and presence of the PBRs, but asserted that the large age uncertainties in the PBRs (10-70kyrs) needed resolution before any firm conclusions could be made from the findings. Such age uncertainties are unacceptably large, given that they allow for the PBRs to have experienced anything from nil to many Dunstan Fault earthquakes. Not surprisingly, our present study is an effort to obtain considerably more age constraints than in the pilot study. Presentation and discussion of these new results are the basis of this report, including assessment of the applicability of PBR studies in the humid-temperate New Zealand environment, and to similar environments in the USA.

## 2. GEOLOGIC SETTING

The Clyde site is located on a remnant of the Central Otago peneplain, a surface of low relief and formed in Cretaceous to Tertiary times when New Zealand was tectonically stable (e.g. McSaveney & Stirling, 1992). The peneplain was developed on the Haast Schist, an areally extensive suite of Mesozoic metasediments and metavolcanics (e.g., Turnbull, 1981). The peneplain was traversed by rivers, lakes and the sea during the late Cretaceous to mid Tertiary, and the degree of chemical weathering of remnants of these cover sediments and underlying schists indicates that conditions were tropical-humid for at least some of this time period. The peneplain was later uplifted and exhumed as a result of contractional tectonism in the late Tertiary and Quaternary to produce the distinctive Central Otago range and basin topography (Stirling, 1991; McSaveney & Stirling, 1992). The exhumed peneplain surface is preserved across most of central Otago due to the virtual absence of Pleistocene glaciation in the region, giving the ranges a distinctively smooth appearance. The smooth peneplain remnants are only interrupted by schist tors and associated PBRs (Fig. 1), and the occasional sarson stone boulders, the extremely hard silicified (silcrete) remnants of the Tertiary cover sediments. The tors are considered to be the products of differential erosion of the schist from the exhumed peneplain surface, and are thought to have been exposed for $10^5$ years or more (e.g., Fahey, 1981; Stirling, 1991). Reverse faults such as the Dunstan Fault are responsible for uplift of the ranges such as the Dunstan Mountains, to the northeast of the Clyde site (Fig. 2).

## 3. COSMOGENIC $^{10}$BE DATA

We here document cosmogenic in-situ $^{10}$Be concentrations and associated laboratory analyses for 11 rock samples taken from the Clyde site, (Appendix 1), Eight of these come from the surface of the Clyde-6 PBR alone, two are from a neighbouring tor, and one is from a large silicified sarson stone nearby (Fig. 3). We here document the analytical work undertaken to obtain exposure ages and erosion rates for the Clyde site.

Surface exposure dating (SED) using cosmogenic isotopes is routinely applied to geomorphology. The basic premise of the method is the buildup of rare isotopes in surface rocks exposed to constant bombardment by cosmic rays. Present-day measurement of the concentration of one or several isotopes, with knowledge of the *in situ* production rate, allows one to constrain the exposure and/or burial history of the rock from where the sample was taken. A good introduction to the method is given by Allègre, (2008; pg 131). Here we apply the SED method in the form that is analytically the simplest and most viable, this being the measurement of the $^{10}$Be concentration in quartz. The method involves taking rock samples, several kilograms each, and extraction of only the $^{10}$Be atoms that were produced *in situ*, from ca. 100 gram of quartz, via physical and chemical means (Child, et al. 2000), performed at the University of Canterbury, New Zealand. Measurement of $^{10}$Be/$^{9}$Be ratios was done via Accelerator Mass Spectrometry (AMS) at GNS Science, New Zealand (Zondervan, et al. 2007).

The sampling positions on the Clyde-6 PBR and neighboring tor are shown in Fig. 3. Eight rock samples were taken from the top and side surfaces of the Clyde-6 PBR alone (Fig. 3). In an attempt to determine when the PBR became precarious, three of these eight samples were taken from the pedestal of the PBR. A vertical transect of two samples were taken from the top of the tor to obtain information about the evolution of shielding of cosmic rays due to attenuation by surrounding rock. Details of the sample processing and measurement are given in Appendix 1, and results are shown in Table 1.

Table 1 Sample results: $^{10}$Be concentration in quartz, attenuation, zero-erosion exposure age, and steady-state erosion rate. Zero attenuation equates to an attenuation correction factor of 1. Exposure age and erosion rate values are quoted with two types of 1-sigma errors, separated by a backslash: the 1st is without the uncertainty in the production rate, while the 2nd one includes it. Attenuation and production rate modeling are discussed in the text.

| ID# | $^{10}$Be conc. [$10^3$ $g_{qtz}^{-1}$] | depth interval [cm] | attenuation correction [] | zero-erosion exposure age [ka] | steady-state erosion rate [mm ka$^{-1}$] |
|---|---|---|---|---|---|
| 1 | 623±7 | 0 – 3 | 0.975±0.002 | 74±1\4 | 7.92±0.10\0.5 |
| 2 | 369±5 | | 0.58±0.21 | 73±27\27 | 8±3\3 |
| 3 | 337±8 | | 0.53±0.24 | 73±33\33 | 8±4\4 |
| 4 | 331±7 | | 0.52±0.24 | 73±34\34 | 8±4\4 |
| 5 | 232±7 | | 0.36±0.32 | 74±66\66 | 8±8\8 |
| 6 | 338±5 | | 0.53±0.24 | 73±33\33 | 8±4\4 |
| 7 | 382±8 | | 0.60±0.20 | 73±25\25 | 8±3\3 |
| 8 | 392±7 | | 0.61±0.20 | 74±24\24 | 8±3\3 |
| 9 | 1037±15 | 0 - 2 | 0.983±0.002 | 123±1.8\7 | 4.69±0.08\0.3 |
| 10 | 952±13 | 4 - 7 | 0.911±0.009 | 122±2.0\7 | 4.74±0.09\0.3 |
| 11 | 6756±47 | 0 - 2 | 0.983±0.002 | 965±7\57 | 0.488±0.009\0.07 |

Table 1 lists the minimum exposure ages and maximum erosion rates, based on measured $^{10}$Be/$^{9}$Be ratios, modelled production rates, and modelled local cosmic-ray attenuation factors. The ages reflect the period of cosmic-ray exposure to the present, calculated on the assumption that no material between the sampled surface and the atmosphere was removed during that interval (zero erosion). Introducing the assumption of surface erosion increases the exposure age as the production rate in the sampled material would have been lower due to attenuation of the cosmic ray intensity by previously overlying (now eroded) material. Therefore the values in Table 1 are only minimum ages for the original (uneroded) surface. The second assumption embodied in the calculation of minimum ages is that the sampled feature started its exposure history without $^{10}$Be from any previous exposures (zero inheritance). Consideration of inheritance decreases the exposure age as only a proportion of the measured $^{10}$Be atoms would have been produced since exposure. Clearly, both assumptions need to be evaluated before we can interpret our analytical results with confidence. Our cosmogenic and geomorphological observations of the Clyde-6 PBR may not be comprehensive enough to reconstruct a detailed evolution in terms of exhumation and erosion towards present-day precariousness. However, it is informative to consider the other extreme of maximum erosion rates, even though the equations for applying the single cosmogenic isotope method allow multiple solutions (Gosse and Phillips, 2001). The basic assumption used in assessing maximum erosion rates is that the rate by which $^{10}$Be is produced, at a certain depth below the eroding surface, equals its disappearance due to erosion and radioactive decay (commonly referred to as steady-state erosion or erosional steady state). Its usefulness is in providing a maximum allowable value for the rate of erosion, albeit at the expense of information about the true exposure age. The two extreme interpretations are mutually exclusive in the sense that they cannot simultaneously represent the actual exposure-erosion history. The minimum age assumes no erosion and the maximum rate assumes an infinitely long exposure.

To calculate the production rate of $^{10}Be$ for surface rock at the site (45.19°S, 169.28°E, 580 m elevation), we use the time-invariant version of Stone's model for spatial scaling (Stone, 2000). Assuming the present day geomagnetic latitude (49.36°S, using IGRF-10) applies for the whole exposure period, we derive a production rate for the Clyde-6 site of (8.83±0.52) $^{10}Be$ atoms $g_{qtz}^{-1}$ $a^{-1}$. The relative error is set to be equal to that of the production rate at high latitudes and sea level: (5.1±0.3) $^{10}Be$ atoms $g_{qtz}^{-1}$ $a^{-1}$. Exposure ages and erosion rates in Table 1 incorporate this relative error. Topographic shielding by nearby hills and mountains is estimated to be less than 1% and has therefore not been considered in the calculations.

In Table 1, the column with attenuation correction factors is a mixture of estimated and calculated values. Only samples ID#1, 9, 10, 11 have simple planar geometries and sufficiently defined vertical sampling depth intervals from which the attenuation of cosmic rays within and above the sample can be calculated. The calculation has the purpose of deriving the effective production rate for the whole of each sample. The calculated attenuation correction includes only that fraction of the cosmic ray flux that is responsible for the production of $^{10}Be$ by spallation of target nuclei, and not the muon-capture component as the latter is only significant at great depths. The single-exponential depth dependence of spallogenic production is characterized by a depth scale of 160 g $cm^{-2}$ (Gosse & Phillips, 2001) which, in combination with an assumed rock density of 2.7 g $cm^{-3}$, is used to calculate the amount of attenuation for each sample. The uncertainty on the correction factors for samples ID# 1, 9, 10, and 11 are assumed to be 10% of the amount of attenuation and to be randomly distributed. Samples ID# 9 and 10 provides a consistency check on the attenuation calculation: The good agreement between these two after correction provides confidence in our application of the method and we can regard these samples as replicates of the same exposure history.

Samples ID# 2 – 8 are sampled across a more complex geometry than the top of the PBR or tor, and consequently we do not have a method available to derive attenuation. The geometrical complexity is the product of differential erosion (sculpting). The schist rockmass of the study area shows considerable heterogeneities in strength properties due to the strong metamorphic foliation and lithological variations that led to the sculpting of tors and PBRs into the irregular shapes seen today. In order to discern vertical and horizontal erosion differences, the degree of attenuation is tuned for each of the samples ID# 2 – 8 individually to yield the same extreme-case values (minimum age, maximum erosion) as that of ID# 1, which is the only sample on the Clyde-6 PBR with a simple planar geometry. The uncertainty on these poorly constrained attenuation values is conservatively estimated as 50% of the amount of attenuation. It is clear that the lack of methodology for samples ID# 2 – 8 hampers straightforward interpretation of how the PBR has developed into the present shape.

## 4. INTERPRETATION OF $^{10}BE$ DATA IN GEOMORPHIC CONTEXT

Interpretation of the data is limited to those samples taken closest to present-day surfaces, and with a simple planar geometry for which the attenuation and erosion is readily described by existing SED methodology (Gosse and Phillips, 2001). Only samples ID#1, 9, and 11 satisfy this criterion. To estimate the extent of vertical erosion for each of these samples, we make use of prior knowledge of how schist lithology has influenced exposure history. A landform evolution study of Bennett et al (2006) in a neighbouring central Otago range demonstrated that the minimum exposure ages for schist are significantly and systematically younger that those of sarson stones. They explained the age discrepancy as being due to the schist eroding much faster than the sarson stones. The correlation between rock type and minimum exposure age thus strongly suggests that slowly eroding surfaces of sarson stones can be used to determine the duration of cosmogenic exposure, and that our apparent exposure ages for the schist only provides constraints on erosion. The $^{10}Be$ data of the three top surface samples can thus be interpreted as a set of one exposure age plus two erosion rates, and we represent the extremes given in Table 1 as Model A values in Table 2.

Table 2 Model reconstructions of the Clyde-6 samples with planar exposure geometry: exposure ages T and erosion rates ε. The models are explained in the text.

| T \ ε [ka] \ [mm ka$^{-1}$] | ID# | 1 | 9 | 11 |
|---|---|---|---|---|
| | rock type | schist | schist | silcrete |
| | feature | top of PBR | top of tor | top of sarson |
| model | | | | |
| A | | ∞ \ 7.92 | ∞ \ 4.69 | 965 \ 0 |
| B | | 965 \ 4.99 | 965 \ 4.68 | 965 \ 0 |
| C | | 964 \ 8.60 | 1075 \ 4.90 | 1077 \ 0 |

Our second model, Model B, assumes: (i) that the three samples were exposed for the same duration; (ii) that the erosion of the silcrete sarson stone is negligible, and (iii) that the original surface of the schist (i.e. prior to the differential erosion that produced Clyde-6 and neighbouring tor) was constant across the less-than-10m distance between the PBR and neighboring tor. In this respect the height difference between PBR and tor (c. 0.3 m) would imply that the PBR has been vertically eroded at a rate different to that of the tor. We reiterate that, for all the models presented here, we assume that there has been no *in situ* $^{10}Be$ inherited from previous exposure, and that the removal of the overlying Tertiary sediment and weathered schist occurred rapidly compared to the erosion of the schist exposed today at the Clyde site. This is a reasonable assumption, given that exposures of the schist peneplain surface where the schist-Tertiary contact is still preserved generally reveal the schist and sediments at the contact (i.e. excluding sarson stones) to be deeply weathered and thus considerably weaker than the schist exposed at the Clyde site (e.g. Stirling 1990, 1991). Furthermore, we construct model B with the assumption that the PBR has been eroded at different rates during two subsequent stages, in order to determine how well the vertical erosion of this feature is constrained by the data. With these assumptions in place, the SED equations have unique numerical solutions for the common exposure age, erosion rate of the tor (sample ID# 9) and average erosion rate of the PBR, but are under-determined with respect to the rate and duration of the two erosion stages for the PBR. From the one finite exposure age and two finite (average) erosion rates, the total amount of eroded schist can be calculated as 4.5 m for the tor, and 4.8 m for the PBR. The implied erosion rates are of the order 0.5cm/kyr, similar to rates derived from a ensemble of environments and methods (e.g. Rapp, 1960; Bishop et al. 1984, Bennett et al. 2006), including from within central Otago. For instance, Bishop et al. (1984) showed that similar rates of catchment denudation are presently occurring in the nearby Falls Dam catchment area, based on sediment volumes accumulated since the dam was constructed. The results of the Falls Dam study supports the conclusion that the erosion rates derived from the $^{10}$Be data are realistic estimates of true schist erosion rates at the Clyde site. We show which pairs of vertical erosion rates for the PBR are permitted by the assumptions and observations of Model B in Fig. 4.

Our third model (Model C) values in Table 2 are exposure age and erosion rate pairs for samples ID# 1, 9, and 11. These are evaluated with the time-varying production scaling model of Desilets and Zreda (2003) and Desilets et al. (2006) as implemented by the CRONUS-Earth calculator (Balco et al., 2008), and assuming a nearly equal exposure age for all three samples. Model C's most significant result is that it suggests that about 3m more schist was removed from above the PBR than from the tor.

The uncertainties in the resulting values for all three models are likely to be large. In this respect Model A uses the least advanced model for geographical scaling of the production rate. Model B has the additional weakness in that muon-capture is not taken into account explicitly: Only $^{10}$Be production through nuclear spallation in quartz is used to construct the set of equations from which solutions were derived. Model C does not have the limitations of Models A and B, and is our preferred model, with a common exposure age of c. 1000kyr and erosion rates for the schist bedrock after removal of the soft and deeply weathered material above.

Schist erosion rates of the order 0.5cm/kyr are perhaps further supported by independent evidence from soils buried by schist slabs shed from the Clyde-6 PBR. Calibrated radiocarbon dates from bulk soil samples are 5400 $\pm$ 40 years BP near the base of the 50cm soil profile (GNS Science NIC lab pers comm.; Fig. 5). This is consistent with the PBR being a Holocene feature, based on the assumption that the soils reflect the present geomorphic processes. It is acknowledged, however, that radiocarbon dates obtained for bulk soil samples are often fraught with uncertainty due to the unknown amount of carbon cycling that has taken place in the soil-atmosphere system. Accordingly, major pre-treatment was carried out on the soil samples prior to radiocarbon dating, so these uncertainties have been minimized as much as possible.

## 5. EVOLUTION OF PBRS IN THE CONTEXT OF NEAR-FIELD DUNSTAN FAULT EARTHQUAKES

Having obtained estimates of the exposure age and vertical erosion rates of the Clyde-6 PBR and nearby tor, and having modelled how schist erosion rates might have varied through time, we now have an idea as to how rapidly unstable schist landforms might develop in the temperate New Zealand environment. Despite the imprecise attenuation factors for side-samples ID# 2-8, the SED results appear to be consistent with that of the top-sample ID# 1. The PBR erosion rate average is 0.5cm/kyr (Model B), and it is possible that its erosion accelerated in a later stage of the ~1000kyr exposure. From this we infer that, anywhere on the present-day surface of the PBR, the rate of schist removal is not less than 0.5cm/kyr, and at the start of the Holocene the PBR would have been ~5 cm larger on all sides (Fig. 6). Given the added stability this extra rockmass would have given to the PBR it is likely that the

Clyde-6 PBR only developed the present precariousness in the Holocene. In the context of the location of the Clyde site near the Dunstan Fault and the $^{10}$Be-derived erosion rates for the Clyde-6 PBR (Table 2), it is possible that few or no Dunstan Fault earthquakes have shaken the PBR in the present form at the Clyde site. Analyses by Stirling and Anooshehpoor (2006) show that the PBR is expected to be shaken down by a PGA of less than 0.2g, which from quick examination of relevant attenuation models appears to be less than half of the median PGAs expected from large Dunstan Fault earthquakes. PBRs at the Clyde site possibly form in the time between major earthquakes and are either shaken down by the major earthquake and/or become eroded to such an extent that they become unstable and topple without the assistance of earthquake shaking. For the rest of central Otago, the importance of earthquake-induced PBR destruction would depend on location, as PBRs located away from active faults would be mainly destroyed by erosion, whereas near-fault PBRs would be destroyed by both strong shaking and erosion. The PBRs may therefore be in a time-independent state of creation and destruction in the former areas, but destruction in the latter areas could also be punctuated by periodic strong shaking.

## 6. COMPARISON WITH WESTERN USA PBR STUDIES

The wider implications of the Clyde PBR results are that the PBRs are much younger than counterparts in arid environments of the western USA. The humid-temperate environment and schist geology of the central Otago region has apparently led to erosion rates of the order 0.5cm/kyr, rates that will have significantly altered the bedrock landforms over time. Despite the limited relevance of our results to arid environments in the western USA and elsewhere, it is worth noting that the results could be relevant to metamorphic terranes in humid-temperate environments in the western USA (e.g. parts of Central California and Pacific Northwest) and elsewhere, where PBR dating has not yet been undertaken. The extrapolation of our New Zealand-based results to these regions may be more appropriate than extrapolations from nearby arid environments.

## 7. CONCLUSIONS

We have constrained the age of precariously-balanced rocks (PBRs) within a metamorphic terrane and humid-temperate environment in New Zealand using in-situ cosmogenic isotopes and geomorphic interpretation. Cosmogenic in-situ $^{10}$Be concentrations from 11 samples of schist and silcrete from the Clyde PBR site in the central Otago region imply rock surface erosion rates of the order 0.5cm/kyr, consistent with rates of landform evolution and catchment denundation determined elsewhere in the region. The PBRs may have reached their precarious state less than 10kyr ago, and may not have experienced any earthquakes on the nearby Dunstan Fault in the present states of precariousness, given the long recurrence interval of the fault (8kyr). Future New Zealand-based efforts should therefore move to studying fragile geomorphic features close to faults with much shorter recurrence intervals (100-1,000 years). The main international contribution arising from our results is that PBRs from metamorphic terranes in humid-temperate environments similar to that of central Otago (e.g. parts of central California and Pacific Northwest) may be considerably younger than counterparts in the arid western USA. In other words PBRs evolve more rapidly in temperate environments than in desert environments, at least for areas of similar lithology to that of central Otago.

## 8. ACKNOWLEDGEMENTS

Thanks go to Matthew Gerstenberger, Tony Hurst, Matthew Purvance and Rasool Anooshehpoor for reviewing the manuscript on which this report is based. We are indebted to Rob Spiers and Sacha Baldwin-Cunningham for their efforts in preparing rock samples for cosmogenic dating under a tight timeframe, and to Jamie Schulmeister for prioritizing and facilitating the work. The research benefited greatly from discussions with Matthew Purvance, Jim Brune, Rasool Anooshehpoor, John Anderson, Lesley Perg, Lisa Grant-Ludwig, Jamie Shulmeister, Russ Van Dissen, Kelvin Berryman, David Barrell, Dylan Rood and Derek Fabel. Lewis Stirling and Toby Stirling are thanked for their enthusiastic assistance in the field. Funding from the Earthquake Commission (EQC), Southern California Earthquake Center (SCEC Contribution number 1265), and Foundation for Research, Science and Technology are gratefully acknowledged.

## 9. REFERENCES

Allègre, C.J. (2008) *Isotope geology*, Cambridge Press.

Balco, Stone, J., Lifton, N., Dunai, T. (2008) A complete and easily accessible means of calculating surface exposure ages or erosion rates from 10Be and 26Al measurements. *Quaternary Geochronology* (in press).

Bell, J.W., J.N. Brune, T. Liu, M. Zreda, and J.C. Yount (1998). Dating of precariously-balanced rocks in seismically-active parts of California and Nevada, *Geology* ***26***, 495-498.

Bennett, E., Youngson, J., Jackson, J., Norris, R.J., Raisbeck, G., and Yiou, F. (2006). Combining geomorphic observations with in situ cosmogenic isotope measurements to study anticline growth and fault propagation in central Otago, New Zealand. *New Zealand Journal of Geology and Geophysics* **49**, 217-231.

Bishop, D.G., Lindqvist, J.K., Ritchie, D.D., Turnbull, I.M. (1984). Modern sedimentation at Falls Dam, upper Manuherikia River, Central Otago, New Zealand. *New Zealand Journal of Geology and Geophysics* **27**: 305-312.

Brune, J.N. (1996). Precarious rocks and ground motion maps for southern California. *Bulletin of the Seismological Society of America* **86**, 43-54.

Child, D., Elliott, G., Mifsud, C., Smith, A.M., and Fink, D. (2000). *Sample processing for earth science studies at ANTARES, Nuclear Instruments and Methods in Physics Research Section B: Beam Interactions with Materials and Atoms,* 172 (1-4), October, 856-860,

Desilets, D., and Zreda, M., (2003) Spatial and temporal distribution of secondary cosmic-ray nucleon intensities and applications to in situ cosmogenic dating. *Earth and Planetary Science Letters* ***206***, 21-42

Desilets, D., Zreda, M., Almasi, P., and Elmore D. (2006) Determination of cosmogenic $^{36}$Cl in rocks by isotope dilution: innovations, validation and error propagation. *Chemical Geology* ***233,*** 185-195

Fahey, B.D. (1981). Origin and age of the upland schist tors of Central Otago, New Zealand. *New Zealand Journal of Geology and Geophysics* **24**, 399-413

Gosse, J. C., Phillips, F. M. (2001) Terrestrial in situ cosmogenic nuclides: theory and application. *Quaternary Science Reviews* **20**, 1475-1560.

McSaveney M.J., and M.W. Stirling, (1992). Central Otago, Basin and Range Country. In Soons J.M. and Selby, M.J. *Landforms of New Zealand*. Second Edition.

Purvance, M.D., Anooshehpoor, R., and Brune J.N. (2008). Freestanding block overturning fragilities: Numerical simulation and experimental validation. *Earthquake Engineering and Structural Dynamics* **37(5),** 791-808.

Rapp, A. (1960). Recent development of mountain slopes in Karkevagge and surroundings, northern Scandinavia. *Geografiska Annaler* **41**: 34-48.

Stirling, M.W. (1990). The Old Man Range and Garvie Mountains: tectonic geomorphology of the Central Otago peneplain, New Zealand. *New Zealand Journal of Geology and Geophysics,* ***33***, 233-244.

Stirling, M.W. (1991). Peneplain modification in an alpine environment of Central Otago, New Zealand. *New Zealand Journal of Geology and Geophysics* ***34***, 195-202.

Stirling, M.W., McVerry, G.H., and Berryman, K.R., (2002). A new seismic hazard model for New Zealand. *Bulletin of the Seismological Society of America* **92**, 1878-1903.

Stirling, M.W. and R. Anooshehpoor (2004). Use of precariously-balanced rocks to test the New Zealand seismic hazard model: a pilot study. *GNS client report* ***2004/158.***

Stirling, M.W. and R. Anooshehpoor (2006). Constraints on probabilistic seismic hazard models from unstable landform features in New Zealand. *Bulletin of the Seismological Society of America* ***96,*** 404-414

Stone, J.O. (2000) Air pressure and cosmogenic isotope production. *Journal of Geophysical Research,* ***105(B10),*** 23,753–23,759.

Turnbull, I.M. (1981). Contortions in the schist of the Cromwell District, Central Otago, New Zealand. *New Zealand Journal of Geology and Geophysics* ***24***, 65-86

Zondervan, A., Poletti, M., Purcell, C.R., Sparks, R.J., (2007). *Accelerator and beamline upgrades at the AMS facility of GNS Science, New Zealand Nuclear Instruments and Methods in Physics Research Section B: Beam Interactions with Materials and Atoms,* 259 (1), 47-49).

## FIGURES

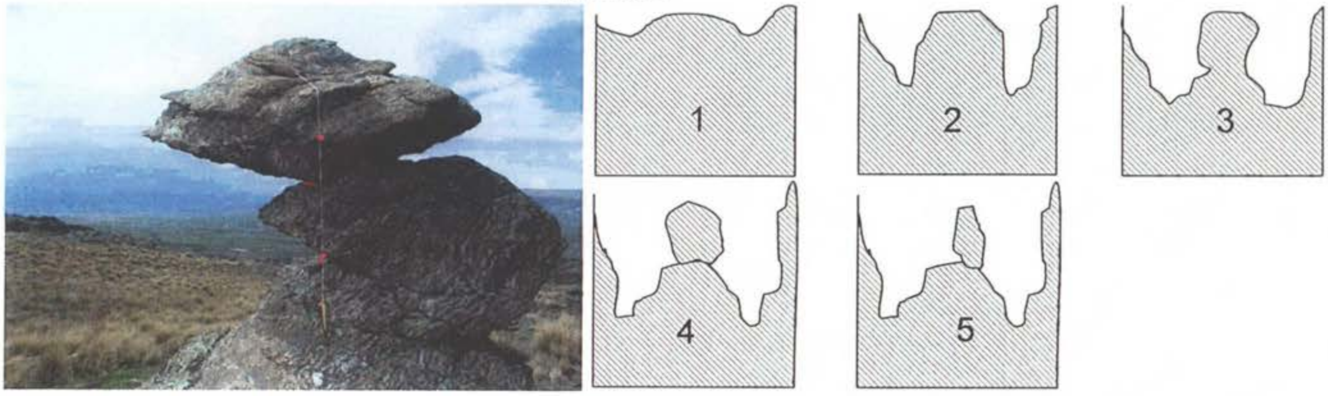


Figure 1 Example of a precariously balanced rock (PBR) in the central Otago region of New Zealand (height of rock about 2m), and a five stage schematic diagram to show how a PBR would develop over time. Note that at stage 4 of the diagram, weathering of the sides of the outcrop has caused the top to break off and form the PBR, and by stage 5 the PBR has become even more precarious (i.e. increasing precariousness as a function of time). For information on the estimation of PBR fragility (ground motions necessary to topple the PBRs) see Stirling & Anooshehpoor (2004, 2006).

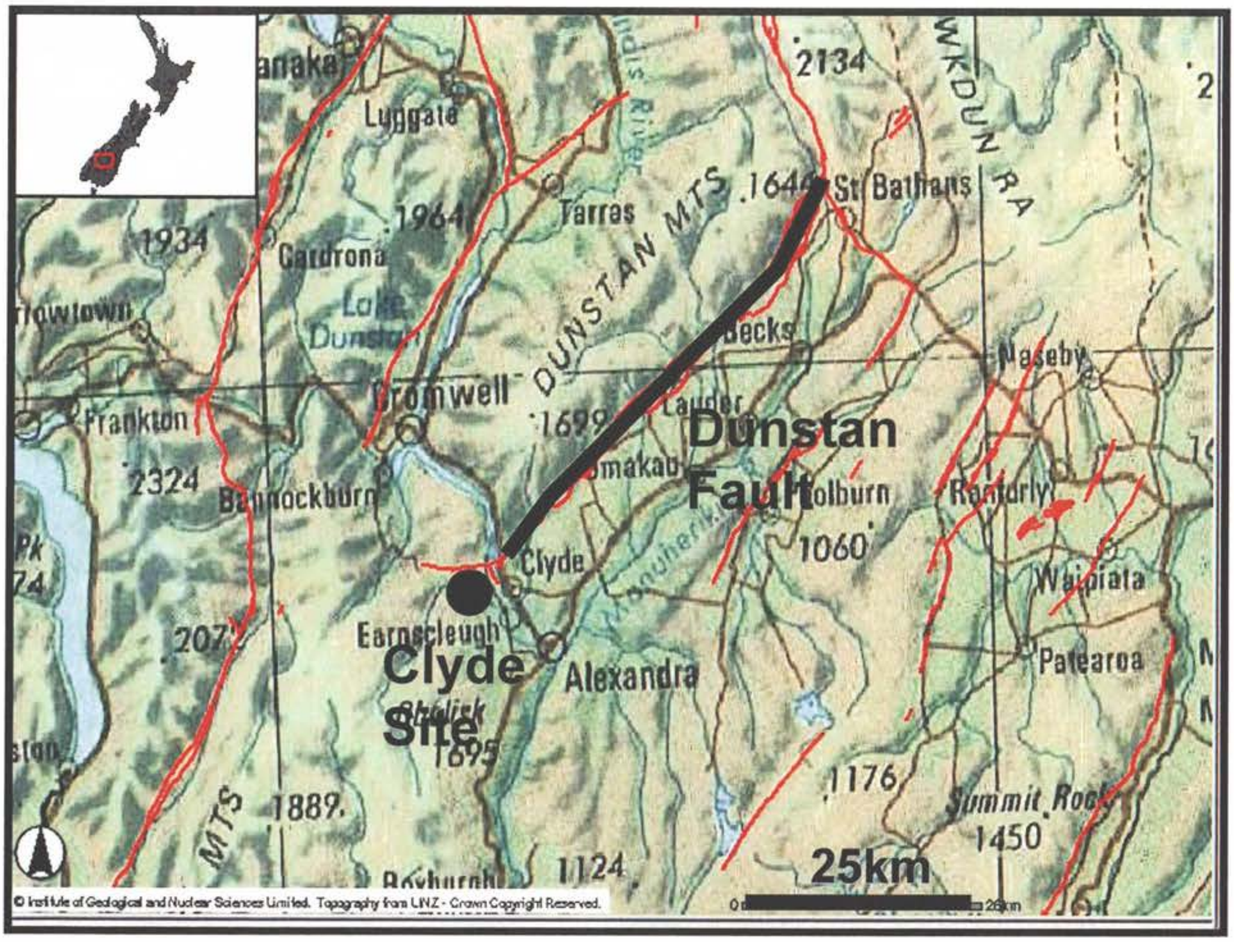


Figure 2 Location of the Clyde site of precariously-balanced rocks (PBR; solid circle) in relationship to the Dunstan Fault (thick black line). Numerous PBR and semi PBRs are present in the approximately 3x3km area of the site (see images in Stirling & Anooshehpoor, 2006).


Figure 3 Location of samples taken for cosmogenic dating, sample IDs, and apparent $^{10}$Be ages (in kyrs). See the text for further explanation.

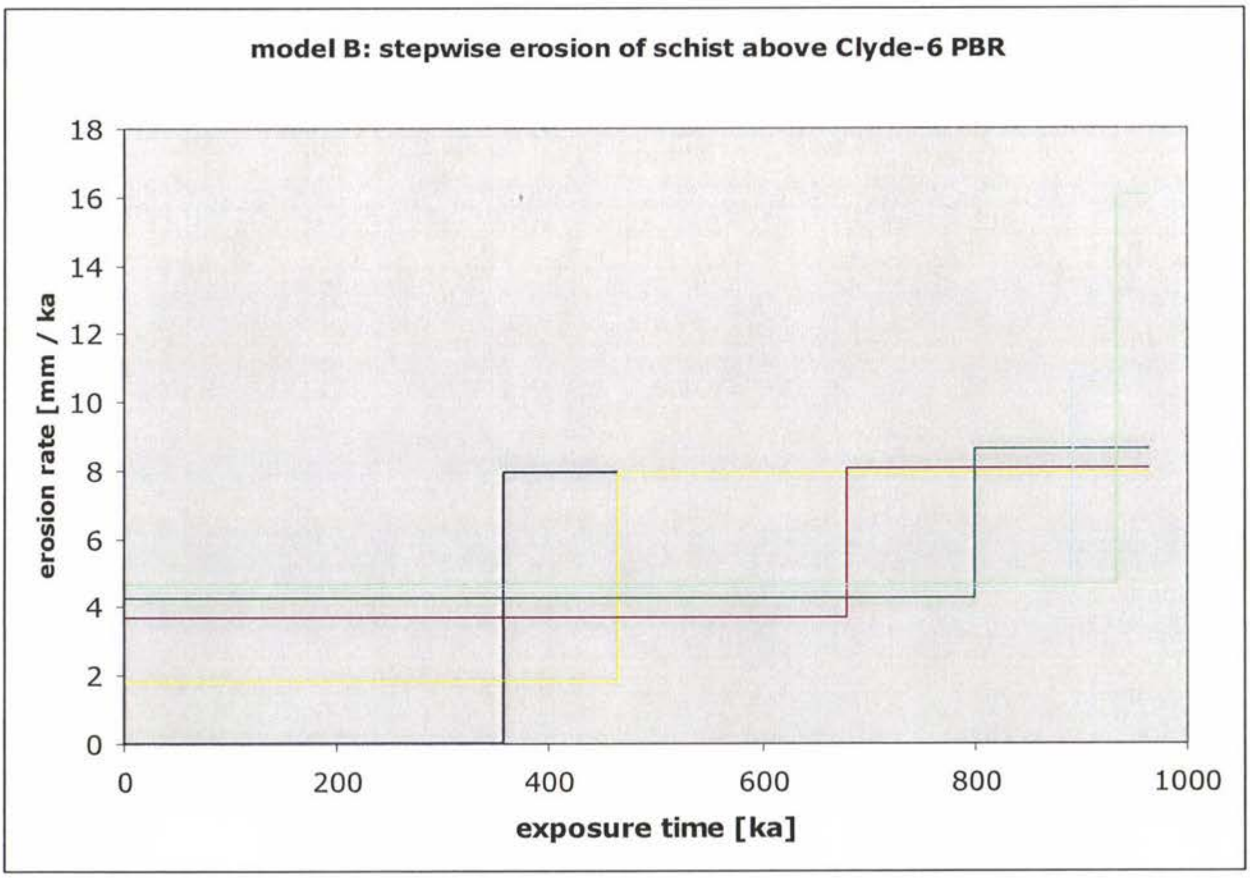


Figure 4 Erosion rate – time graphs for surfaces sampled in this study (assuming Model B).

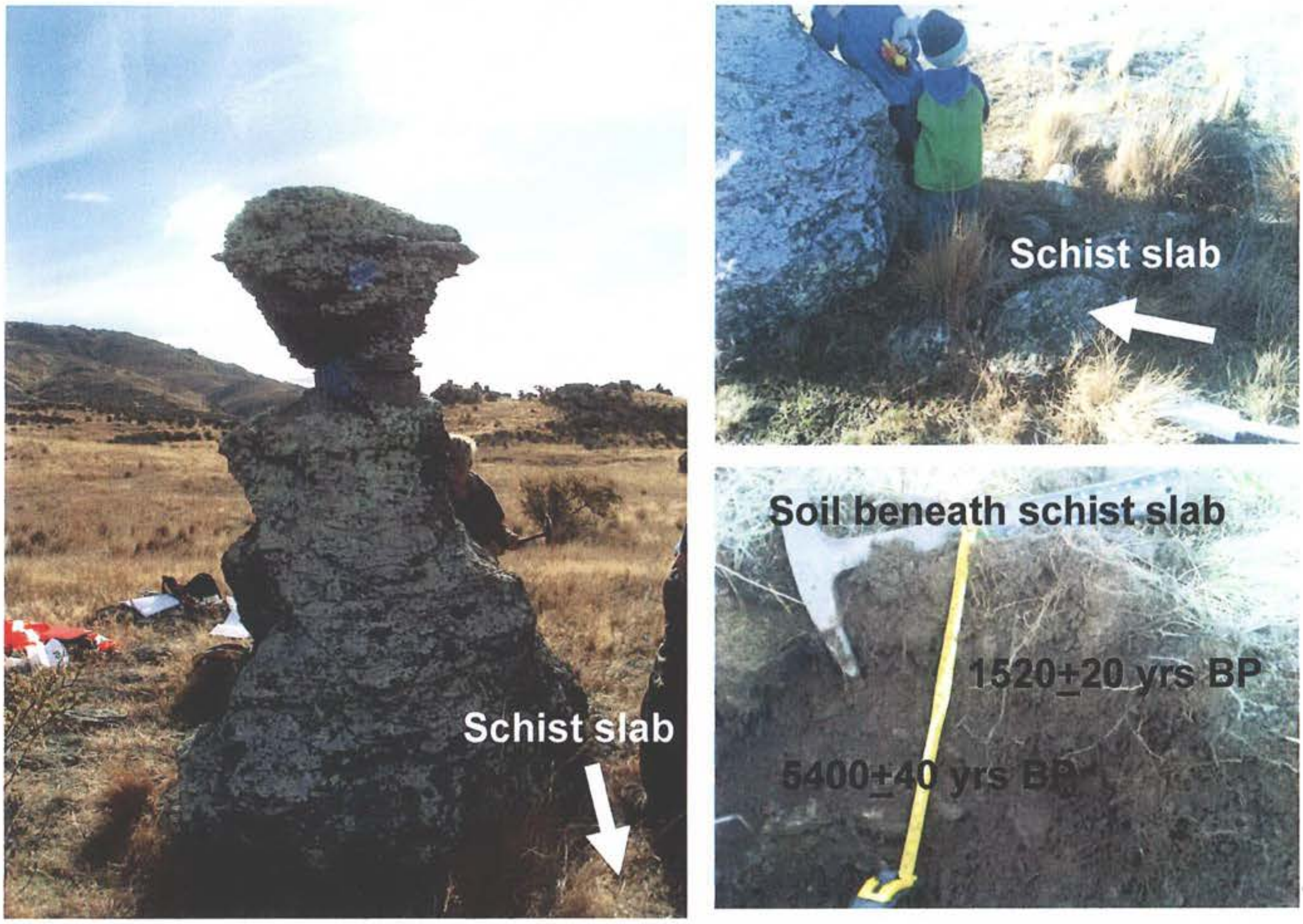


Figure 5 Calibrated radiocarbon dates for soils buried beneath a schist slab derived from Clyde-6. The length of the tape measure shown in the image is 50cm.

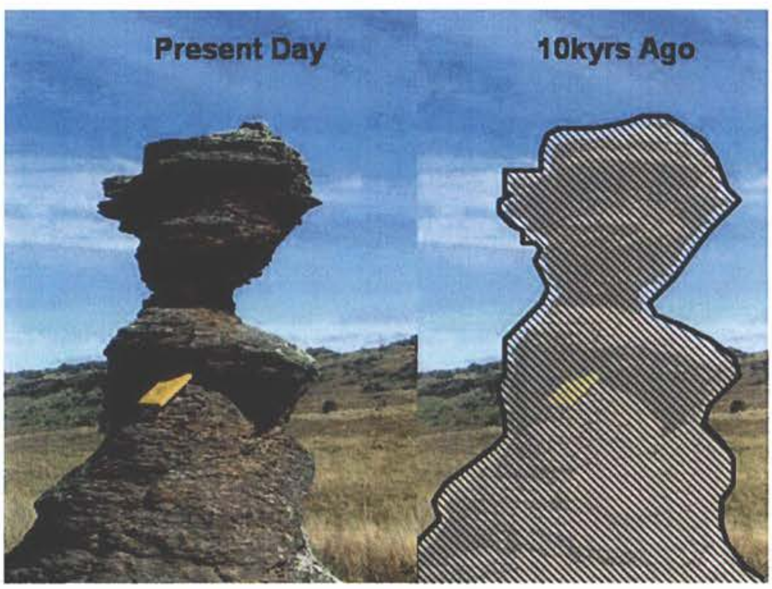


Figure 6 Hypothetical 10kyr profile for Clyde-6 assuming that the erosion rates shown in Table 2 have in operation over the Holocene. The 10kyr profile does not consider additional modifications due to shedding of slabs from the PBR (see Fig. 5). See the text for further explanation

# APPENDICES

## APPENDIX 1 COSMOGENIC DATA

Appendix 1. Sample details: identifiers, key chemical pretreatment parameters, $^{10}Be$ AMS results. The measured isotopic ratios and associated 1-sigma errors are given as percentages of the $^{10}Be$ standard used, NIST SRM4325.

| ID# | field# | R# | NZ# | weight [$g_{qtz}$] | $^{9}Be$ carrier [mg] | carrier yield [%] | Be# | $^{10}Be/^{9}Be$ ratio [% NIST] |
|---|---|---|---|---|---|---|---|---|
| 1 | T10 | 30060 | 318 | 100.13 | 0.4036 | 133 | 2869 | 7.58±0.08 |
| 2 | T3 | 30052 | 311 | 110.32 | 0.4096 | 61.5 | 2861 | 4.89±0.07 |
| 3 | T4 | 30053 | 312 | 79.94 | 0.4024 | 45 | 2862 | 3.30±0.07 |
| 4 | T5 | 30055 | 313 | 105.05 | 0.4032 | 142 | 2864 | 4.25±0.08 |
| 5 | T6 | 30056 | 314 | 90.03 | 0.3986 | 81 | 2865 | 2.59±0.07 |
| 6 | T9 | 30059 | 317 | 95.11 | 0.3995 | 102 | 2868 | 3.96±0.05 |
| 7 | T8 | 30058 | 316 | 80.06 | 0.3973 | 99 | 2867 | 3.79±0.08 |
| 8 | T7 | 30057 | 315 | 80.18 | 0.4058 | 142 | 2866 | 3.81±0.06 |
| 9 | T1 | 30050 | 309 | 70.27 | 0.4067 | 71 | 2859 | 8.79±0.13 |
| 10 | T2 | 30051 | 310 | 90.29 | 0.4094 | 53 | 2860 | 10.29±0.14 |
| 11 | S11 | 30061 | 307 | 80.09 | 0.4986 | 129 | 2870 | 53.1±0.4 |
| chemistry blank | | 30054 | 319 | 0 | 0.4016 | 72 | 2863 | 0.03±0.02 |
| AMS blank | | | | | | | 1463 | 0 (by def.) |

| | Sampling | | | | Physical prep | | | Chemical prep | | | |
|---|---|---|---|---|---|---|---|---|---|---|---|
| field id | mineral type | locality | longitude / latitude | elevation [m] | R number | by whom ? | NZ number | chemical separation | pure quartz [g] | Be carrier [mg] | Be yield [%] |
| UPenn blank | | | | | | | | RGD | | | |
| T1 | schist | beside Clyde6 | 169.2814E /45.1911S | 580 | 30050 | RS (CU) | 309 | RS (CU) | 70.27 | 0.4067 | 71 |
| T2 | schist | beside Clyde6 | 169.2814E /45.1911S | 580 | 30051 | RS (CU) | 310 | RS (CU) | 90.29 | 0.4094 | 53 |
| T3 | schist | Clyde6 | 169.2814E /45.1911S | 580 | 30052 | RS (CU) | 311 | RS (CU) | 110.32 | 0.4096 | 61.5 |
| T4 | schist | Clyde6 | 169.2814E /45.1911S | 580 | 30053 | RS (CU) | 312 | RS (CU) | 79.94 | 0.4024 | 45 |
| blank | | | | | 30054 | RS (CU) | 319 | RS (CU) | 0 | 0.4016 | 72 |
| T5 | schist | Clyde6 | 169.2814E /45.1911S | 580 | 30055 | RS (CU) | 313 | RS (CU) | 105.05 | 0.4032 | 142 |
| T6 | schist | Clyde6 | 169.2814E /45.1911S | 580 | 30056 | RS (CU) | 314 | RS (CU) | 90.03 | 0.3986 | 81 |
| T7 | schist | Clyde6 | 169.2814E /45.1911S | 580 | 30057 | RS (CU) | 315 | RS (CU) | 80.18 | 0.4058 | 142 |
| T8 | schist | Clyde6 | 169.2814E /45.1911S | 580 | 30058 | RS (CU) | 316 | RS (CU) | 80.06 | 0.3973 | 99 |
| T9 | schist | Clyde6 | 169.2814E /45.1911S | 580 | 30059 | RS (CU) | 317 | RS (CU) | 95.11 | 0.3995 | 102 |
| T10 | schist | Clyde6 | 169.2814E /45.1911S | 580 | 30060 | RS (CU) | 318 | RS (CU) | 100.13 | 0.4036 | 133 |
| S11 | granite | near Clyde6 | 169.2814E /45.1911S | 580 | 30061 | RS (CU) | 307 | RS (CU) | 80.09 | 0.4986 | 129 |

## AMS measurement

| UPenn | Be number | BeW / pos | 10/9 [NIST] | error | 10/9 [at/at] | error | error [%] | 10Be [106 at] | error | 10Be [103 at/g] | error | error [%] |
|---|---|---|---|---|---|---|---|---|---|---|---|---|
| blank | 1463 | 138 / 6,26,36 | | 0 | 0 | 0 | 0 | | | | | |
| T1 | 2859 | 138 / 4,22 | 0.0879 | 0 | 3E-12 | 3.9E-14 | 0.0144 | 73.097756 | 1.0561 | 1037.086 | 15.25 | 0.0147 |
| T2 | 2860 | 138 / 23 | 0.10292 | 0 | 3E-12 | 4.1E-14 | 0.0131 | 86.156612 | 1.1301 | 951.7654 | 12.68 | 0.01332 |
| T3 | 2861 | 138 / 7,27 | 0.04887 | 0 | 1E-12 | 2.1E-14 | 0.0141 | 40.930145 | 0.5779 | 369.0032 | 5.488 | 0.01487 |
| T4 | 2862 | 138 / 8,28 | 0.033 | 0 | 1E-12 | 2.2E-14 | 0.0218 | 27.152693 | 0.5924 | 336.8899 | 7.748 | 0.023 |
| blank | 2863 | 138 / 10,29 | 0.00027 | 0 | 8E-15 | 6.7E-15 | 0.8148 | 0.2217167 | 0.1807 | | | |
| T5 | 2864 | 138 / 12,32 | 0.04249 | 0 | 1E-12 | 2.5E-14 | 0.0193 | 35.030654 | 0.676 | 331.3559 | 6.661 | 0.0201 |
| T6 | 2865 | 138 / 13,33 | 0.02591 | 0 | 8E-13 | 2.2E-14 | 0.0274 | 21.117656 | 0.5787 | 232.0997 | 6.734 | 0.02901 |
| T7 | 2866 | 138 / 14,34 | 0.03813 | 0 | 1E-12 | 1.9E-14 | 0.016 | 31.638788 | 0.5062 | 391.8318 | 6.703 | 0.01711 |
| T8 | 2867 | 138 / 16 | 0.03792 | 0 | 1E-12 | 2.4E-14 | 0.0211 | 30.805473 | 0.6499 | 382.0105 | 8.426 | 0.02206 |
| T9 | 2868 | 138 / 17,37 | 0.03962 | 0 | 1E-12 | 1.6E-14 | 0.0131 | 32.364749 | 0.4248 | 337.9564 | 4.853 | 0.01436 |
| T10 | 2869 | 138 / 18,38 | 0.07583 | 0 | 2E-12 | 2.4E-14 | 0.0103 | 62.579661 | 0.6437 | 622.7698 | 6.677 | 0.01072 |
| S11 | 2870 | 138 / 19,39 | 0.53094 | 0 | 2E-11 | 1.1E-13 | 0.007 | 541.30086 | 3.7824 | 6755.889 | 47.28 | 0.007 |

## Exposure calculations

| UPenn | pressure [hPa] | Stone's prod-rate [atoms/(g*a)] | error | shielding correction | error | depth [cm] | attenuation correction | error | zero-erosion exposure age [ka] | error | sample descript |
|---|---|---|---|---|---|---|---|---|---|---|---|
| blank | | | | | | | | | | | |
| T1 | 945.483 | 8.5475965 | 0 | 1 | 0 | 2 | 0.9838 | 0.0016187 | 126.96 | 1.878237 | top of neighbour closest to Clyde-6 |
| T2 | 945.483 | 8.5475965 | 0 | 1 | 0 | 3 | 0.914 | 0.0085977 | 125.36 | 2.043991 | beneath T1 |
| T3 | 945.483 | 8.5475965 | 0 | 1 | 0 | 0 | 0.976 | 0.012 | 44.687 | 0.862347 | uppermost, on side, ~35cm from top |
| T4 | 945.483 | 8.5475965 | 0 | 1 | 0 | 0 | 0.976 | 0.012 | 40.762 | 1.062988 | mid-upper, side, ~30 cm down from T3 |
| blank | | | | | | | | | | | |
| T5 | 945.483 | 8.5475965 | 0 | 1 | 0 | 0 | 0.976 | 0.012 | 40.086 | 0.944616 | mid-lower, side, ~60 cm below T4 |
| T6 | 945.483 | 8.5475965 | 0 | 1 | 0 | 0 | 0.976 | 0.012 | 28.001 | 0.882282 | lowermost, side, ~60 cm below T5, ~5 cm above ground |
| T7 | 945.483 | 8.5475965 | 0 | 1 | 0 | 0 | 0.976 | 0.012 | 47.482 | 1.000277 | outermost one-third rind of shoulder of pedestal |
| T8 | 945.483 | 8.5475965 | 0 | 1 | 0 | 0 | 0.976 | 0.012 | 46.279 | 1.168607 | middle one-third rind of shoulder of pedestal |
| T9 | 945.483 | 8.5475965 | 0 | 1 | 0 | 0 | 0.976 | 0.012 | 40.892 | 0.773061 | innermost one-third rind of shoulder of pedestal |
| T10 | 945.483 | 8.5475965 | 0 | 1 | 0 | 0 | 0.9759 | 0.0024149 | 75.971 | 0.835949 | top of Clyde-6 |
| S11 | 945.483 | 8.5475965 | 0 | 1 | 0 | 2 | 0.9838 | 0.0016187 | 1002.3 | 7.20603 | top of a sarson stone outcrop nearby |

## APPENDIX 2 SPREADSHEET OF CALCULATED EROSION RATES ASSUMING APPARENT (SATURATED) $^{10}$BE AGE

| P0 (production rate at/g/a)=4.53 | L (adsorption length cm)=150 | lamda (decay const)=5.17E-07 | density (g/cc)=2.7 | |
|---|---|---|---|---|
| **t (apparent age in yr)** | **N (no of atoms)** | **erosion rate(g/cm2/a)** | **erosion rate (cm/a)** | Fig. 3 ref and field id |
| 76000 | 3.38E+05 | 1.94E-03 | 7.17E-04 | 1 (T10) |
| 45000 | 2.01E+05 | 3.29E-03 | 1.22E-03 | 2 (T3) |
| 41000 | 1.84E+05 | 3.62E-03 | 1.34E-03 | 3 (T4) |
| 40000 | 1.79E+05 | 3.71E-03 | 1.37E-03 | 4 (T5) |
| 28000 | 1.26E+05 | 5.32E-03 | 1.97E-03 | 5 (T6) |
| 41000 | 1.84E+05 | 3.62E-03 | 1.34E-03 | 6 (T9) |
| 46000 | 2.06E+05 | 3.22E-03 | 1.19E-03 | 7 (T8) |
| 47000 | 2.10E+05 | 3.15E-03 | 1.17E-03 | 8 (T7) |
| 127000 | 5.57E+05 | 1.14E-03 | 4.23E-04 | 9 (T1) |
| 125000 | 5.48E+05 | 1.16E-03 | 4.30E-04 | 10 (T2) |

www.gns.cri.nz

Principal Location

1 Fairway Drive
Avalon
Lower Hutt 5010
PO Box 30368
Lower Hutt 5040
New Zealand
T +64-4-570 1444
F +64-4-570 4600

Other Locations

Dunedin Research Centre
764 Cumberland Street
Dunedin 9016
Private Bag 1930
Dunedin 9054
New Zealand
T +64-3-477 4050
F +64-3-477 5232

Wairakei Research Centre
114 Karetoto Road, Wairakei
Taupo 3377
Private Bag 2000
Taupo 3352
New Zealand
T +64-7-374 8211
F +64-7-374 8199

National Isotope Centre
30 Gracefield Road, Gracefield
Lower Hutt 5010
PO Box 31312
Lower Hutt 5040
New Zealand
T +64-4-570 1444
F +64-4-570 4657